DOI: https://doi.org/10.15407/techned2025.03.031

TORQUE OF A SLOTLESS AXIAL-FLUX PERMANENT MAGNET TORQUE MOTOR WITH SOLID SLITTED STATOR YOKE

I.S. Petukhov*, V.G. Kireyev, K.P. Akinin***, Ye.V. Isaiev**
Institute of Electrodynamics National Academy of Sciences of Ukraine,
Beresteiskyi Ave., 56, Kyiv, 03057, Ukraine.
E-mail: igor_petu@ukr.net.

A three-phase slotless torque motor of axial structure with permanent magnets and a solid stator core is considered. The effect of the circular slits in the core, that prevent the flow of eddy currents, is investigated. It is noted that the magnetic field of the stator winding has a minimum effect on the field created by permanent magnets and it can be neglected. Two stages of the study are defined: the first stage is the determination of the maximum torque in a static state, and the second stage is the determination of losses from motional eddy currents during the movement of the stator core relative to the rotor. The field problem is solved using the software "COMSOL Multiphysics". A smooth analytical function is used to approximate the magnetization curve of core steel. It is demonstrated by simulation of the physical model that the application of four slits can reduce the torque loss approximately by a factor of 4 or increase likewise the maximum rotational speed of the rotor. References 8, figures 9, table 1.
Keywords: torque motor, permanent magnets, solid stator core, slitted core.

Introduction. A torque motor (TM) is an electric synchronous or DC machine, the mode of operation of which is low rotational frequency, turning at a definite angle and stalling for a certain time providing the nominal value of the torque on the shaft. A decrease in rotational speed can be realized by using a gear reducer. In any case, ensuring a static mode with the creation of a nominal shaft torque during the given period requires the design of an electric machine for exactly such a mode, regardless of available or non-available reduction gear. The TM functionality is often limited to angle of rotation with less than a single revolution. In such a case, the TM is referred to as an “actuator” [1, 2].

With the advent of permanent magnets (PM) based on samarium and, especially, neodymium, the interest in the use of small direct-action slotless electric drives has increased. Although the slotless design has slightly lower weight-and-size indicators compared to the traditional slotted design [3], it is technologically simple and, very importantly, has less torque ripple. For slotless electric machines, it is not necessary to follow the pole ratio, which is essential for slotted machines with laminated stator cores [4]. In many cases, the requirements for the simplicity of the design and its cheapness are decisive factors. This applies to the release of a large series of devices under the conditions of low manufacturing costs, or the creation of a small quantity of devices under the conditions of rapid production preparation.

In some applications, the axial-flux PM motor (AFPMM) exhibits better weight-to-size ratios than traditional radial-flux PM motors [5]. AFPMM can conveniently accommodate a fairly large number of poles. Therefore, they are well accepted for low-speed applications. In some cases, the high moment of inertia becomes useful for applications where AFPMM also combines the properties of a flywheel. The small frequency of rotation, and, accordingly, the small frequency of the magnetic field in the magnetic core of TM causes the moderate losses in steel from eddy currents. Taking this fact into account makes it possible to manufacture the stator magnetic core (actually a yoke, since a slotless design is being considered) without using the traditional for industrial frequency laminated structure. In this approach, the yoke is made solid from of cheap steel, and the thin annular through-slits are made to reduce the influence of eddy currents [6]. However, there is a problem with the effectiveness of this method depending on the number and location of the slits [6]. That is, it is necessary to determine the permissible reduction of the torque and the corresponding range of rotational speed for the specified load torque of the electric drive.

ORCID: * https://orcid.org/0000-0003-1416-1174; ** https://orcid.org/0000-0002-9407-1074;
*** https://orcid.org/0000-0002-7830-2311

Thus, the paper's **purpose is to study the influence of the annular slits and their location in solid stator yoke on the torque value of the slotless axial-flux PM motor**.

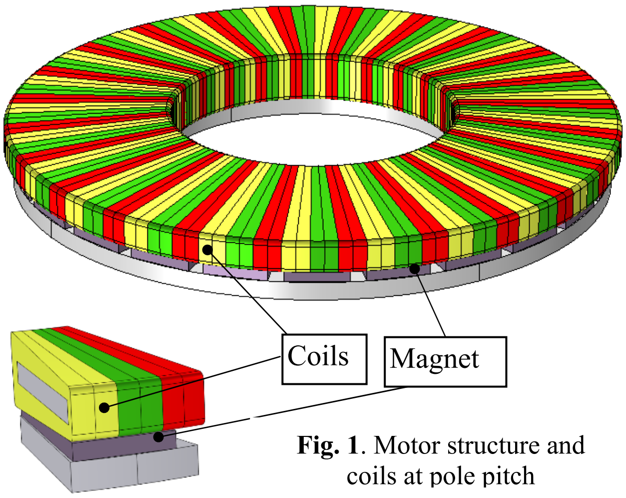

Fig. 1. Motor structure and coils at pole pitch

Motor structure. The study of TM with radial structure was carried out in [1]. The technical applications with direct drive often require minimization of the axial dimension of the device. In this case, the advantages of AFPMM play a decisive role when choosing this type of machine. Fig. 1 presents the design of a 24-pole AFPMM and the fragment representing a pole pitch with phase coils (yellow – *A*, green – *B*, red – *C*). The geometric dimensions of the active zone and some parameters of the motor's physical model are given in Table. It should be noted that such a winding design is not optimal from the point of view of coil manufacturing technology with such a large number of poles, but it provides the maximum torque value. Following the concept of [6], let us consider the annular slits in the stator magnetic core, which consists only of the yoke (Fig. 1). To ensure the strength of the structure, the slits cannot be extended over the entire circumference. Similar to the solution in the paper [6], the "bridges" in adjacent slits are located with a symmetrical displacement (Fig. 2).

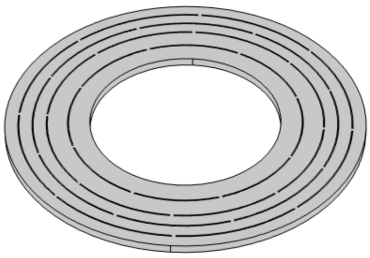

Fig. 2. Stator core with four slits

Since the influence of the winding on the distribution of the magnetic field in the stator magnetic core is small compared to the field of PM, it can be neglected when calculating the losses from eddy currents in the stator core. Due to the large non-magnetic gap between the magnetic cores of the stator and rotor, the eddy currents from the magnetic field pulsations in the rotor and PM can also be neglected. Note that the specified rotor speed of the motor (Table) should not exceed 3.5 rad/s. Accordingly, the frequency of the supply current can be up to 6.7 Hz (the angular frequency ω is up to 42 rad/s). Then the study can be divided into two stages. The first stage is the calculation of the maximum torque with the rotor stopped. In the second stage, the braking torque due to motional eddy currents in the solid stator core is calculated ignoring the currents in the winding.

Mathematical model and software. The formulation of the field problem is based on the following assumptions:

- neglecting the "bridges" in the stator core that interrupt the slits;
- neglecting the the influence of winding currents on the magnetic state of the stator core;
- neglecting the eddy current losses in the PM and rotor core;
- the maximum torque does not depend on the combination of the supplied stator phases.

The determination of the maximum torque with the rotor stopped corresponds to the magnetostatic problem. The torque can be determined by calculating the Maxwell stress tensor τ_M or by integrating the Lorentz force F_L over the relevant domains. The Maxwell tensor is expressed in terms of the vectors of the magnetic field strength *H* and magnetic flux density *B* using the expression [7]:

Parameter	Value	Value/τ
Pole pairs, p	12	-
External diameter, D_a (mm)	340	10
Internal diameter, D_i (mm)	180	5.3
Middle pole pitch, τ (mm)	34	1
Cores width, L_z (mm)	80	2.35
Height of stator yoke, h_{ys} (mm)	8	0.24
Winding thickness, h_w (mm)	5	0.147
Effective air gap, h_w+δ (mm)	5.5	0.162
Magnet height, h_m (mm)	6	0.18
Angular magnet width, α_m (°)	140	-
Height of rotor yoke, h_{yr} (mm)	10	0.24
Current density, J_w (A/mm^2)	5	-
Permanent flux density, B_r (T)	1,3	-
Rated angular velocity, ω_R (rad/s)	3.5	-

$$\mathbf{n}\tau_M = -1/2\,\mathbf{n}(\mathbf{H}\cdot\mathbf{B}) + (\mathbf{n}\cdot\mathbf{H})\mathbf{B}^T\,, \tag{1}$$

where n is the normal to the surface of the body on which the force acts, $(\cdot)^T$ is the transposition symbol.

The torque $\mathbf{T}$ is calculated by integrating the tensor (1) over the surface Ω covering the stator or rotor:

$$\mathbf{T} = \oint_{\partial\Omega} (\mathbf{r}-\mathbf{r}_0)\times(\mathbf{n}\,\tau_M)\,dS\,, \tag{2}$$

where $\partial\Omega$ is a surface enclosing the domain Ω; $\mathbf{r}$ is the radius-vector of an arbitrary point; $\mathbf{r}_0$ is the radius vector of the point on the axis of rotation.

Let us assume that the axis of rotation coincides with the z-axis. Then the projection of the torque on the axis of rotation is

$$T_z = \mathbf{e}_z \cdot \mathbf{T}\,. \tag{3}$$

The Lorentz force $\mathbf{F}_L$ is calculated in domains with current as the vector product of the current density vector $\mathbf{J}$ and the magnetic flux density vector $\mathbf{B}$:

$$\mathbf{F}_L = \mathbf{J}\times\mathbf{B}\,. \tag{4}$$

The torque in this case is determined as the integral over the winding area Ω_w:

$$T_z = \int_{\Omega_W} (\mathbf{r}/|\mathbf{r}|)\times\mathbf{e}_\varphi F_{L\varphi}\mathbf{e}_z d\Omega\,, \tag{5}$$

where $\mathbf{e}_\varphi$ and $\mathbf{e}_z$ are the unit vectors of the cylindrical coordinate system (r, φ, z).

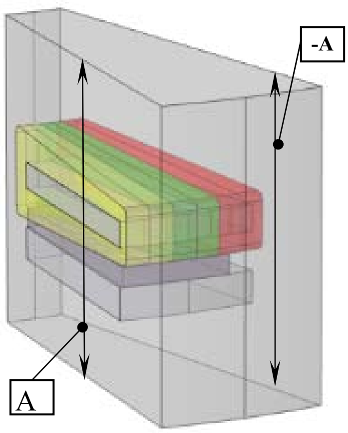

Fig. 3. Modelling domain for solving the magnetostatic boundary value problem, boundaries with antiperiodic conditions

A. First Stage. Magnetostatic Field.

Expressions (1) – (4), as well as the expression for the component of the Lorentz force included in expression (5) are implemented in the corresponding interfaces of the «COMSOL Multiphysics» software package, which was used for modelling. The first stage corresponds to a magnetostatic problem with external currents in the winding phases. This problem is formulated with respect to the magnetic vector potential $\mathbf{A}$ in the interface «Magnetic Fields». The computational domain for the first stage of modelling is shown in Fig. 3. Since due to symmetry only one pole pitch can be considered, the boundary conditions on the lateral boundaries (corresponding to the axial sections) satisfy the antiperiodic condition (Fig. 3). The conditions of magnetic insulation are set on the remaining boundaries:

$$\mathbf{n}\times\mathbf{A} = 0\,. \tag{6}$$

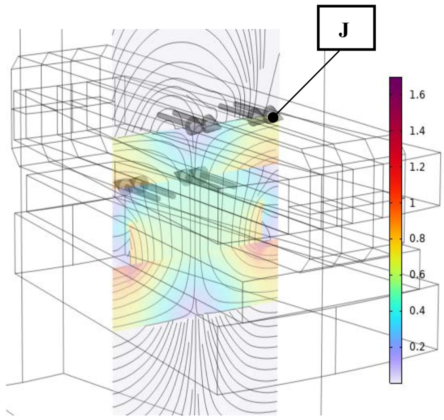

Fig. 4. Magnetic flux density (norm) in the middle cross section and current flow in phases A, C

Since a three-phase power supply from the inverter is considered, the current always flows through two phases. Therefore, the maximum torque can be achieved with different phase combinations. But such maximums differ very slightly. Based on the above assumption, we will consider the average torque. Thus, according to computation by solving the magnetostatic problem the maximum torque for this motor is 50 N·m. Fig. 4 shows the distribution of magnetic flux density and the direction of the current density of phases A and C in the cross-section corresponding to the average radius of the magnetic core.

B. Second Stage. Magnetic and Electric Field.

In the second stage, as said previously, the winding is disregarded in the analysis. Then the simple form of the stator core allows us to consider the movement of the stator relative to the rotor. The braking torque can be calculated by dividing the losses from eddy currents Q_{rh}, caused by the movement of the conductive medium in the magnetic field, by the angular frequency ω_R:

$$T_Q = Q_{rh}/\omega_R\,. \tag{7}$$

The «Magnetic and Electric Fields» interface was used to solve the problem. In this interface, the three-dimensional boundary value problem is formulated with respect to the magnetic vector potential **A** and the electric scalar potential *V*. As noted above, the influence of the windings on the magnetic field distribution can be neglected. Thus, the modelling area can be considered to consist only of the yokes and the PM, as shown in Fig. 5. It shows the stator yoke segment, divided by four irregular spaced slits. The distance between the slits decreases as the distance from the axis increases to compensate for the increase in torque of a segment. The antiperiodic boundary conditions are the same as in the first stage (Fig. 3).

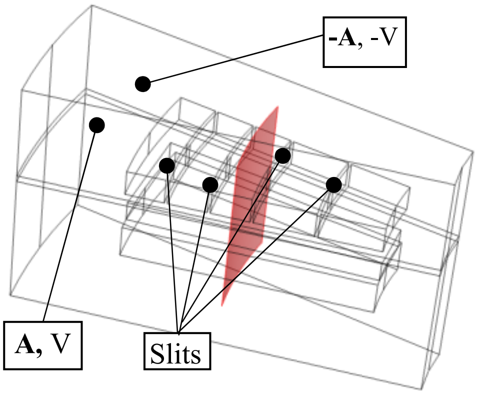

Fig. 5. Domain for simulation of eddy current losses in stator core and central cross section of magnetic core

An important factor for the solution convergence is the smoothness of the steel magnetization curve. One of the magnetization models provided in the COMSOL software is the assignment of relative magnetic permeability. To ensure the smoothness, the dependence of magnetic permeability on the flux density norm was specified as a fractional rational positive function:

$$\mu(|\mathbf{B}|) = 1 + \mu_{\max} \Big/ \left[1 + \left(|\mathbf{B}| / B_S\right)^m\right], \tag{8}$$

where $\mu_{\max}$ is the initial relative magnetic permeability of steel, B_S and m are the coefficients with the corresponding units of measurement. The graph of the dependence $H = B/\mu(B)$ according to (8) and the approximation error from the catalogue data are shown in Fig. 6 for the values $\mu_{\max} = 950$; $B_S = 1.4$; $m = 6.6$. Note that the accuracy of the approximation is critical at high field intensities. The magnetic permeability in this range is significantly reduced. Therefore, the small errors in determining the magnetic permeability in the range of high magnetic flux density lead to significant errors in the torque evaluation.

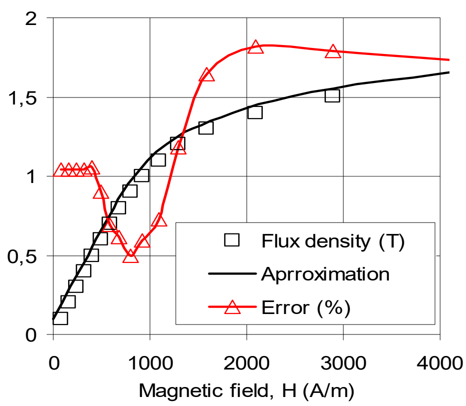

Fig. 6. Magnetization curve and approximation error

When modeling the eddy currents in a ferromagnetic conducting medium, it is important to make the mesh thinner towards the surface through which the field penetrates. This is necessary for accuratemodeling of skin effect. An adequate mesh also contributes to better solution convergence in COMSOL solver. To ensure an acceptable accuracy of field calculation (about 1%), the "field penetration depth" δ should include up to 3 first-order grid elements [8]. In this case, the "field penetration depth" of an unsaturated medium for structural steel with electrical conductivity $\sigma \approx 10^{-7}$ S/m is

$$\delta = \sqrt{2 / \mu\sigma\omega} = \\ = \sqrt{2 / \left(950\,\mu_0 \cdot 10^7 \cdot 226\right)} = 0.84 \text{ (mm)}. \tag{9}$$

Considering that the stator yoke thickness is 8 mm, about 30 uniform mesh elements are required to achieve an accuracy of 1%. The numerical experiments with a densified mesh containing 30 elements along the vertical coordinate allowed us to select the mesh (Fig. 7) for admissible convergence.

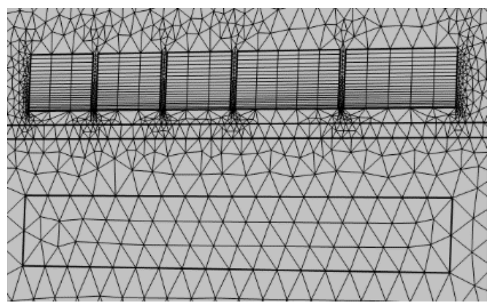

Fig. 7. Mesh on the radial cross section of stator core

Results. The greater the number of slits in the stator yoke, the lower the eddy current losses. However, the width of these slits cannot be less than 0.3…0.5 mm for technological reasons. Therefore, the increase in the number of slits results in the decrease of magnetic flux and, consequently, the reduction of torque. Thus, three variants are studied in the paper: a) single slit, on average diameter; b) two slits dividing the stator yoke into three equal parts; c) the half of the stator yoke closest to the axis divided into 2 equal parts, and the far half divided into 3 equal parts. The location of the slits for variant

c) is shown in Figs. 2, 5, 7. Fig. 5 also shows a fragment of a cylindrical secant surface on which the magnetic field is evaluated. The norm of magnetic flux density and the flux lines are shown for the variant without slits (Fig. 8, *a*) and with four slits (Fig. 8, *b*) for a rotor rotational speed of 30 rpm.

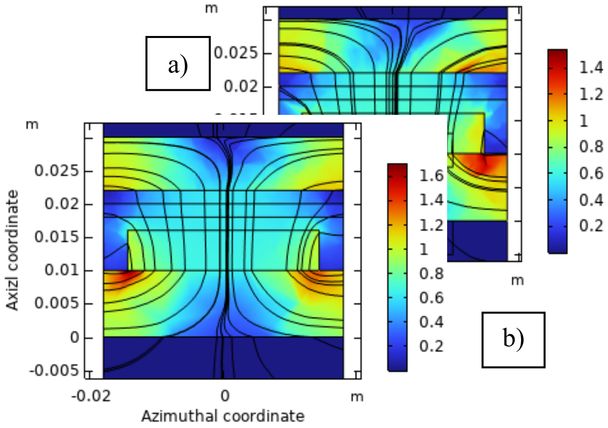

Fig. 8. Norm and streamlines of magnetic flux density (T); *a*) without slits; *b*) four slits

As can be seen, the flux lines for the slitted stator core are less "deformed" by eddy currents in the direction of motion (Fig. 8, *b*), that indicates a lesser influence of eddy currents due to their decrease by the slits. The distribution of magnetic flux density magnitude in both cases (in stator) also indirectly indicates a more uniform magnetic flux distribution in the slitted stator core. When the stator is not slitted, it offers a greater resistance to the total magnetic flux, resulting, as noted above, in a decrease of torque. As can be seen from the field patterns in Fig. 8, the maximum flux density observed in the stator differs by approximately 0.14…0.16 *T*. The highest value takes place in the stator core. In the case of slitted stator, the magnetic flux is greater, that consequently results in greater torque. However, the decrease of magnetic flux in solid stator can be used only as a rough estimation of the reduction in torque, as demonstrated below.

Fig. 9 shows the plots of the percentage torque as a function of the rotational speed for all the stator designs mentioned earlier. Also for the stator design with three slits, the measurement results obtained on the laboratory model are given. The experimental data show 3...5% discrepancy with the calculated data. The braking torque determined by the losses in the stator core (7) are subtracted from the maximum torque determined in the first stage. The linearity of the plots corresponds to the well-known fact that the eddy current losses are proportional to the squared frequency.

According to the simulation results, it can be said that the solid stator core leads to a loss value of 1.2 (%/rpm). In the stator core with one slit located on its average radius, the torque losses are already up to 0.9 (%/rpm). Three slits located evenly across the width of the magnetic core make it possible to reduce this value to 0.5 (%/rpm), and four slits located as described above and shown in Figs. 3, 5, 7 – to 0.3 (%/rpm). In other words, the implementation of four slits allows reducing the torque losses by four times, or at rotor speed of 33 rpm, the torque losses are reduced from 40% to 10% (Fig. 9).

The magnitude of the torque decrease naturally depends on the ratio of the geometric dimensions, the parameters of the ferromagnet, the magnetic field intensity and, especially, the number of pole pairs. However, in today's traditional designs of PM motors, with rare exceptions, PM based on neodymium are always used. The size of the air gap in slotless machines is determined by the current density and the technology's precision. This determines the magnetic flux density in the air gap, the range of which is very narrow. Therefore, based on the theory of similarity of electrical machines, it can be stated that the relative values of the decrease in torque with increasing rotational speed obtained in the paper will be close for machines with corresponding relative width of the stator yoke disk L_δ/τ and its relative height h_{ys}/τ.

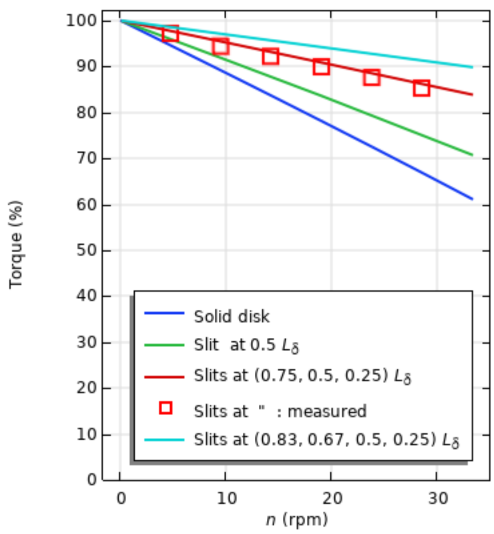

Fig. 9. Torque versus rotational speed

Conclusions. In slotless axial-type TMs, instead of the traditional laminated magnetic core design, it is possible to manufacture a solid stator core at low rated rotational speeds. Such a technological technique can be useful for cost reduction in design and preparation time. However, the high losses are observed in the solid core due to eddy currents. As a result, the torque decreases almost linearly with increasing rotational speed.

The reducing the influence of eddy currents on the torque can be achieved by making a certain number of annular slits in the magnetic core. For example, making four slits at a given rotational speed allows reducing the permissible torque loss by approximately 4 times. On the other hand: at a given permissible torque value, the rotational speed can be increased by the same number of times.

The work was supported by the state project "To develop scientific principles and principles of construction of magnetoelectric mechatronic modules for specialized automatic control systems" ("Mechatron"), KPKVK 6541030.

1. Kireyev V.G., Akinin K.P. Features of the development of slotless brushless magnetoelectric torque motors. *Pratsi Instytutu elektrodynamiky NAN Ukrainy*. 2022. No 63. Pp. 31–39. DOI: https://doi.org/10.15407/publishing2022.63.031.
2. Paulides J.J.H., Meessen K.J., Lomonova E.A. Eddy-Current Losses in Laminated and Solid Steel Stator Back Iron in a Small Rotary Brushless Permanent-Magnet Actuator. *IEEE Transactions on Magnetic*s. 2008. Vol. 44. No 11. Pp. 4373–4376. DOI: https://doi.org/10.1109/TMAG.2008.2001996.
3. Min S.G., Sarlioglu B. Advantages and Characteristic Analysis of Slotless Rotary PM Machines in Comparison With Conventional Laminated Design Using Statistical Technique. *IEEE Transactions on Transportation Electrification.* 2018. Vol. 4. No 2. Pp. 517–524. DOI: https://doi.org/10.1109/TTE.2018.2810230.
4. Jia S., Qu R., Li J., Fan X., Zhang M. Study of Direct-Drive Permanent-Magnet Synchronous Generators With Solid Rotor Back Iron and Different Windings. *IEEE Transactions on Industry Application*s. 2016. Vol. 52. No 2. Pp. 1369–1379. DOI: https://doi.org/10.1109/TIA.2015.2490618.
5. Slutskiy D., Aung S.H., Basnet S. Comparison of Axial and Radial Flux Permanent Magnet Machines. 2022 North American Power Symposium (NAPS), Salt Lake City, UT, USA, 9-11 October 2022. Pp. 1–6. DOI: https://doi.org/10.1109/NAPS56150.2022.10012265.
6. Friedrich L.A.J., Gysen B.L.J., Jansen J.W., Lomonova E.A. Analysis of Motional Eddy Currents in the Slitted Stator Core of an Axial-Flux Permanent-Magnet Machine. *IEEE Transactions on Magnetic*s. 2020. Vol. 56. No 2. Pp. 1–4. DOI: https://doi.org/10.1109/TMAG.2019.2953625.
7. COMSOL multiphysics modeling and simulation software. URL: https://www.comsol.com/documentation (accessed at 20.08.2024).
8. Petukhov I. S. Estimation of the accuracy of calculation by numerical methods of the characteristics of an alternating electromagnetic field with skin effect. *Tekhnichna Elektrodynamika.* 1987. No 1. Pp. 20–25. (Rus)

УДК 621.313.84 : 531.383

ОБЕРТАЛЬНИЙ МОМЕНТ БЕЗПАЗОВОГО МОМЕНТНОГО ДВИГУНА З ПОСТІЙНИМИ МАГНІТАМИ ІЗ КІЛЬЦЕВИМИ ЩІЛИНАМИ У СУЦІЛЬНОМУ ЯРМІ СТАТОРА

І.С. Пєтухов, В.Г. Кірєєв, К.П. Акинін, Є.В. Ісаєв
Інститут електродинаміки НАН України,
пр. Берестейський, 56, Київ, 03057, Україна,
e-mail: igor_petu@ukr.net.

Розглянуто трифазний безпазовий моментний двигун осьової конструкції з постійними магнітами та суцільним осердям статора. Досліджено дію кільцевих щілин в осерді, що перешкоджають протіканню вихрових струмів. Відзначено, що магнітне поле обмотки статора мінімально впливає на поле, створюване постійними магнітами, і цим впливом можна нехтувати. Визначено два етапи дослідження: перший – визначення максимального обертального моменту в статичному стані; другий – визначення втрат від вихрових струмів під час руху статора без обмотки відносно ротора. Польову задачу розв'язували за допомогою програмного забезпечення «COMSOL Multiphysics». Застосовано гладку аналітичну функцію для апроксимації залежності магнітної проникності сталі від магнітної індукції. За допомогою моделювання фізичної моделі було продемонстровано, що використання чотирьох щілин може зменшити втрати обертального моменту приблизно у 4 рази або збільшити максимальну швидкість обертання ротора на таку саму величину. Бібл. 8, рис. 9, табл. 1.

Ключові слова: моментний двигун, постійні магніти, суцільне осердя статора, осердя із щілинами.

Received 17.09.2024
Accepted 28.11.2024